PNAS RESEARCH ARTICLE | NEUROSCIENCE

Distinct oxytocin signaling pathways synergistically mediate rescue-like behavior in mice

Feng-Rui Zhang[a,b,c,1], Juan Liu[a,1], Jieqi Wen[d,e], Zi-Yan Zhang[a], Yijia Li[d,e], Eric Song[a], Li Hu[b,c,2], and Zhou-Feng Chen[a,d,e,f,g,h,2]

Affiliations are included on p. 10.

Edited by Donald Pfaff, Rockefeller University, New York, NY; received November 12, 2024; accepted March 27, 2025

Spontaneous rescue behavior enhances the well-being and survival of social animals, yet the neural mechanisms underlying the recognition and response to conspecifics in need remain unclear. Here, we report that observer mice experience distress when encountering anesthetized conspecifics, prompting spontaneous rescue-like behavior toward the unconscious mice. This behavior facilitates the earlier awakening of anesthetized mice while simultaneously alleviating stress in the helper mice. Our findings reveal that endogenous oxytocin (OXT) release from the hypothalamic paraventricular nucleus (PVN) to the oxytocin receptor (OXTR) in the central nucleus of the amygdala (CeA) regulates the emotional component of rescue-like behavior. In contrast, OXT release from the PVN to OXTR in the dorsal bed nucleus of the stria terminalis (dBNST) mediates the motor component of the behavior. Furthermore, we demonstrate that these two pathways exhibited distinct temporal dynamics and functional roles. The OXT^{PVN}-$OXTR^{CeA}$ pathway is activated in a transient and intense manner, acting as a trigger for rescue-like behavior, whereas the OXT^{PVN}-$OXTR^{dBNST}$ pathway responds in a sustained manner, ensuring the continuation of the behavior. These findings highlight the remarkable ability of rodents to engage in targeted helping behavior and suggest that distinct subcortical oxytocinergic pathways selectively and synergistically regulate the motor and emotional aspects of rescue-like behavior.

rescue-like behavior | anesthesia | oxytocin | amygdala | BNST

Significance

This study reveals that mice exhibit spontaneous rescue-like behavior, facilitating the recovery of anesthetized conspecifics without prior training or external rewards. Observer mice, distressed by their anesthetized peers, instinctively engage in social licking and grooming, which accelerates awakening while also alleviating their own stress levels. This innate response serves as a valuable model for exploring the mechanisms underlying prosocial behavior. Moreover, the research identifies specific neuronal pathways in the brain, driven by the neuropeptide oxytocin, that independently govern the emotional and motor components of this behavior. These findings improve our understanding of the evolutionary roots of empathy and may provide insights into social behavior across species.

Humans are capable of remarkable acts of selfless heroism in life-threatening situations (1). The human instinct to help others has long fascinated scientists across various disciplines (2–5). Spontaneous helping behavior plays a crucial role in strengthening social bonds, fostering reciprocity and cooperation, and enhancing the well-being of social animals (6–10). This behavior integrates multiple components, including sensory, emotional, and motor pathways: Sensory cues convey social information, emotional processes modulate responses, and motor actions execute prosocial behaviors. From an evolutionary perspective, the automatic mirroring of another's affective state—emotional contagion—is essential to empathy-driven helping behavior. It serves as the foundation from which emotional and cognitive empathy evolved sequentially (6, 11). Consequently, growing evidence suggests that the neural mechanisms underlying empathy and prosocial behavior may be evolutionarily conserved, enabling experimental interrogation of the molecular and neural mechanisms (6, 8, 12).

Despite existing challenges (13), recent advances have facilitated the study of prosocial behavior at the molecular and neural levels using rodents as an animal model (8, 14–18). Among various forms of helping behavior, rescue behavior—assisting distressed individuals in life-threatening situations—remains one of the least understood (19, 20). Spontaneous rescue behavior has been documented in a range of nonhuman animal species, including primates (21), wild boars (22), whales (23), birds (24), and ants (25). Rats have also demonstrated the ability to learn and perform helping behavior (26–28). However, reports of spontaneous rescue behavior in nonhuman mammals are rare, primarily based on anecdotal evidence. Whether rodents can exhibit spontaneous rescue behavior without explicit reward is still unknown.

We developed a mouse rescue-like behavioral paradigm to investigate the mechanisms underlying spontaneous rescue behavior. In this paradigm, distressed observer mice exposed to anesthetized conspecifics engage in social licking and grooming, facilitating the anesthetized mice's earlier recovery. We demonstrate that this behavior is mediated by the release of oxytocin (OXT)—a prosocial neuropeptide synthesized in the paraventricular nucleus of the hypothalamus (PVN) (29)—into the central nucleus of the amygdala (CeA) and the dorsal bed nucleus of the stria terminalis (dBNST). These neural pathways regulate emotional processing and allo-licking behavior, respectively. Our findings suggest that

Author contributions: F.-R.Z., J.L., and Z.-F.C. designed research; F.-R.Z., J.L., J.W., Z.-Y.Z., Y.L., and E.S. performed research; F.-R.Z., J.W., and Y.L. contributed new reagents/analytic tools; F.-R.Z., J.L., J.W., Z.-Y.Z., Y.L., and E.S. analyzed data; F.-R.Z., J.L., L.H., and Z.-F.C. wrote response to reviewers; and F.-R.Z., J.L., L.H., and Z.-F.C. wrote the paper.

The authors declare no competing interest.

This article is a PNAS Direct Submission.

[1]F.-R.Z. and J.L. contributed equally to this work.

[2]To whom correspondence may be addressed. Email: huli@psych.ac.cn or chenz@szbl.ac.cn.

This article contains supporting information online at https://www.pnas.org/lookup/suppl/doi:10.1073/pnas.2423374122/-/DCSupplemental.

Published April 23, 2025.

rodents can flexibly assist conspecifics based on their specific needs, underscoring the importance of a comprehensive approach to understanding the origins of prosocial behavior across species.

Results

Mice Perform Rescue-Like Helping Behavior Instinctively. To develop a spontaneous rescue-like behavioral paradigm, we anesthetized the mouse (referred to as demonstrator) via intraperitoneal (i.p.) injection of a ketamine cocktail, a commonly used anesthetic in animal surgery that induces stable anesthesia (30) (Fig. 1*A*). The anesthetized demonstrator was then placed in a testing chamber with a naïve mouse, referred to as the observer. Upon encountering a demonstrator, the observer quickly approached and engaged in vigorous facial licking (primarily targeting the eyes and mouth) and extensive body grooming and licking behaviors toward the demonstrator (Fig. 1 *A*–*D* and Movie S1). To determine whether observers exhibit these behaviors toward comatose animals, we induced a comatose state in demonstrators using high-dose clozapine (31) or chloral hydrate, a sedative-hypnotic (32). Observers also engaged in social licking behavior toward comatose demonstrators (*SI Appendix*, Fig. S1*A*). Notably, observers primarily exhibited licking and grooming behaviors toward live demonstrators rather than dead ones or artificial substitutes (a stuffed mouse resembling a real mouse) (Fig. 1*E* and *SI Appendix*, Fig. S1 *B* and *C*). These findings suggest that mice can distinguish between conspecifics with and without vital signs, and these behaviors are intentionally directed toward live partners. These approaching and allogrooming/licking behaviors (hereafter referred to as social licking) were regarded as targeted helping and prosocial behaviors (16, 17, 33, 34).

Compared with males, females exhibited more facial-licking but less body grooming (Fig. 1*C*), while the total duration of social licking did not differ between sexes (Fig. 1*D*). Although males

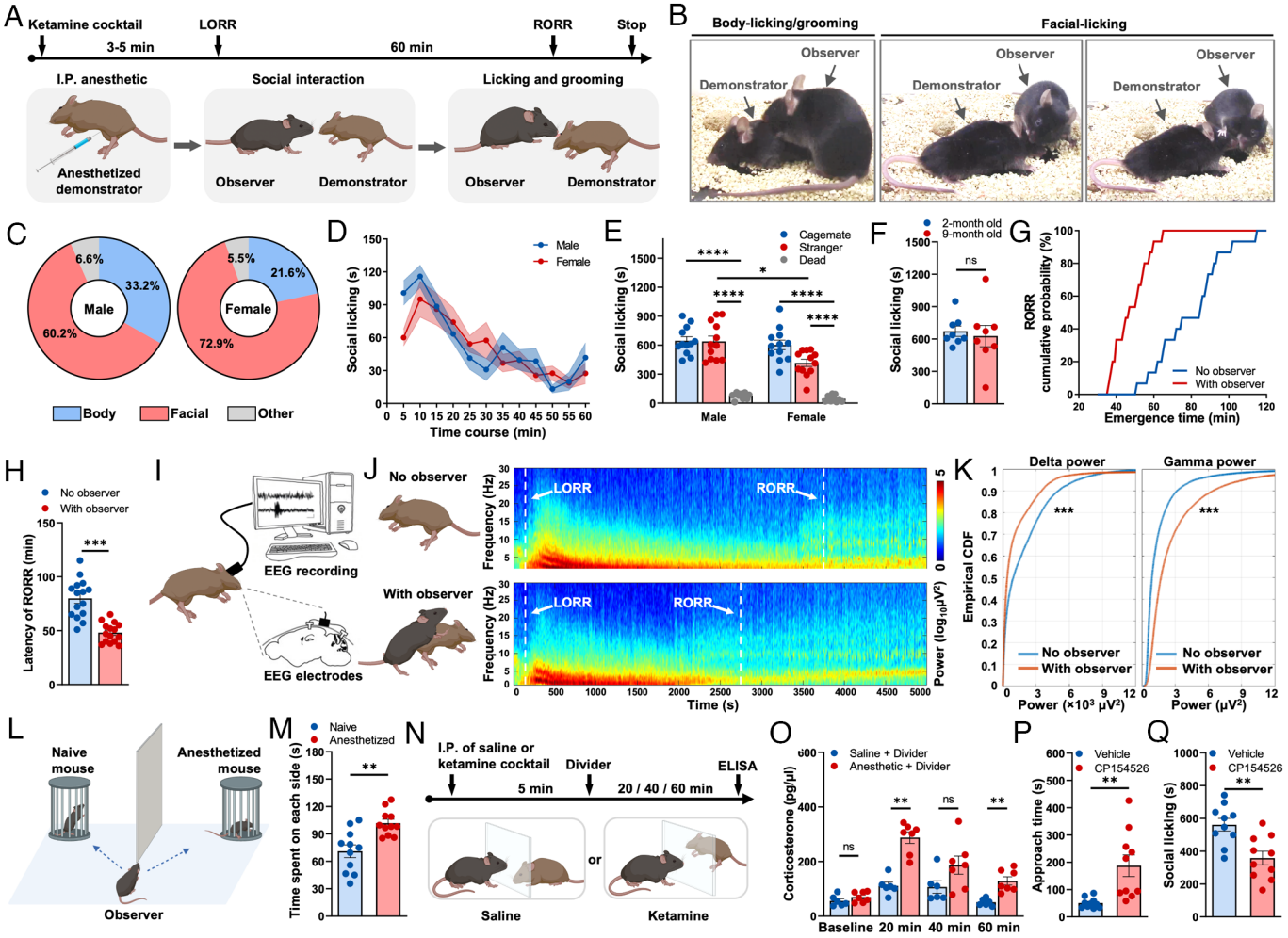

Fig. 1. Mouse rescue-like behavioral paradigm. (*A*) Experimental schematic: showing observer mouse interacts with an anesthetized demonstrator, performing grooming and licking behaviors. LORR and RORR indicate the demonstrator's anesthesia states. (*B*) Representative images of the observer's body-grooming/licking (*Left*) and facial-licking (*Middle*: licking eyes, *Right*: licking mouth). (*C*) The ratio of the subtype of behaviors in male and female observers (n = 12 for each gender). (*D*) Time course of social licking (n = 12 for each gender). (*E*) Social licking time toward the cagemate, stranger, or dead mouse (n = 12 for cagemate and stranger groups; n = 9 for dead group). (*F*) Different ages of observers' social licking time (n = 4 males + 4 females for each group). (*G*) Cumulative probability of demonstrators' RORR latency. (*H*) Demonstrators' RORR latency with and without observers' rescue-like behavior (n = 8 males + 7 females for each group). (*I*) EEG recording schematic. (*J*) Time-frequency spectra of EEG in demonstrator with/without rescue-like behavior. (*K*) Empirical CDF of delta and gamma powers in demonstrators with/without rescue-like behavior (n = 5 for each group, all male). (*L*) Emotional discrimination test schematic. (*M*) Time spent on the side of the anesthetized or naïve mouse (n = 5 males + 6 females). (*N*) Schematic of divider social paradigm. (*O*) Plasma corticosterone levels in the divided-chamber test (n = 6 for saline + divider group, n = 7 for anesthetic + divider group, all male). (*P* and *Q*) Approach (*P*) and social licking time (*Q*) after saline or CP154526 injection (n = 6 males + 4 females for each group). Statistical analyses included paired-sample *t* test (*M*), independent-sample *t* test (*F*, *H*, *P*, and *Q*), two-way ANOVA with Tukey's multiple comparison (*E* and *O*), and independent-sample Kolmogorov–Smirnov test (*K*). **P* < 0.05, ***P* < 0.01, ****P* < 0.001, and *****P* < 0.0001; ns, no significance. Data are means ± SEM. ANOVA, analysis of variance; EEG, electroencephalogram; ELISA, enzyme-linked immunosorbent assay; CDF, cumulative distribution functions; LORR, loss of righting reflex; RORR, resumption of righting reflex.

spent a similar amount of time engaging in social licking with both familiar (cagemates) and unfamiliar (stranger) demonstrators, females exhibited reduced social licking toward strangers (Fig. 1*E*). Social licking behavior in mice aged 2 to 9 mo showed no significant differences (Fig. 1*F*).

These rescue-like behaviors significantly accelerated the resumption of the righting reflex (RORR), a key indicator of recovery from unconsciousness (35) (Fig. 1 *G* and *H*). Electroencephalography (EEG) recordings from the demonstrators further revealed that those receiving social licking transitioned into a shallower anesthetic state, as indicated by reduced delta-band power—a measure of anesthesia depth (36)—accompanied by an earlier recovery of consciousness, as reflected by the rapid restoration of high-frequency power (37) (Fig. 1 *I*–*K*). These findings suggest that social licking facilitates faster emergence from unconsciousness in anesthetized mice. Given the striking resemblance of this behavior to human efforts to resuscitate individuals at risk of dying from loss of consciousness, we refer to it hereafter as "rescue-like behavior."

Rescue-Like Behavior Is Driven by Social Stress. Recognition and contagion of others' emotions are essential for prosocial behavior, with the social transmission of emotional states from distressed demonstrators to naïve observers serving as a key prerequisite (38, 39). To investigate this, we first conducted an emotion discrimination test to determine whether the observers could distinguish anesthetized demonstrators from nonanesthetized counterparts (40) (Fig. 1*L*). We found that the observers spent more time with the anesthetized mice, suggesting their ability to recognize the affective state of the demonstrators (Fig. 1*M*). Next, to assess whether observer mice experienced distress upon exposure to anesthetized mice, we measured corticosterone (CORT) levels in the observer's plasma using a divided-chamber paradigm that prevented observers from physically interacting with the demonstrator (Fig. 1*N*). Compared to naïve mice (saline + divider group), observers interacting with anesthetized mice (anesthetic + divider group) exhibited elevated CORT levels (Fig. 1*O*), indicating their heightened stress levels resulting from exposure to anesthetized demonstrators, and social stress might be a key driver of rescue-like behavior. To further examine this, we administered CP154526, a corticotropin-releasing factor receptor (CRFR) antagonist (41), or vehicle to observers. Remarkably, CP154526 treatment significantly prolonged the approach time (Fig. 1*P*), reduced social licking (Fig. 1*Q*), and impaired the observers' ability to discriminate demonstrators' states (*SI Appendix*, Fig. S1 *D* and *E*). These results indicate that reducing stress levels diminished observers' motivation to perform rescue-like behavior.

Oxytocin of the Paraventricular Nucleus of the Hypothalamus Mediates Rescue-Like Behavior. To investigate the neural mechanism underlying rescue-like behavior, we examined mice lacking the *Oxt* gene, referred to as *Oxt* knockout (*Oxt* KO) mice (*SI Appendix*, Fig. S2*A*), given the well-established role of OXT in social behavior (42–44). Both male and female *Oxt* KO mice showed a delayed approach time and a reduction in social licking duration compared to wild-type (WT) mice. (Fig. 2 *A*–*D*). We then examined the activity of OXT neurons in the hypothalamic paraventricular nucleus (PVN), a key site of OXT synthesis, using fiber photometry in Oxt^{Cre} mice expressing Cre-dependent AAVDJ-Ef1a-DIO-GCaMP6s (Fig. 2*E* and *SI Appendix*, Fig. S2*B*). We observed elevated Ca^{2+} activity in PVN OXT neurons (OXT^{PVN}) when observers approached anesthetized mice (Fig. 2 *F* and *G* and *SI Appendix*, Fig. S2*C*). Furthermore, OXT^{PVN} neurons exhibited a rapid increase in Ca^{2+} transients at the onset of social licking (Fig. 2 *H* and *I* and *SI Appendix*, Fig. S2*D*). To further assess the role of OXT^{PVN} neurons, we chemogenetically inhibited their activity by expressing Cre-dependent virus AAV8-hSyn-DIO-hM4D(Gi)-mCitrine (Gi+) or control virus AAV8-hSyn-DIO-mCitrine (Gi–) into the PVN of Oxt^{Cre} mice via i.p. injection of clozapine (45) (Fig. 2*J* and *SI Appendix*, Fig. S2*E*). Inhibition of OXT^{PVN} neurons significantly delayed the approach time (Fig. 2 *K* and *M*) and impaired social licking (Fig. 2 *L* and *N*) in both male and female mice. These findings indicate that OXT, along with OXT^{PVN} neurons, mediates both the emotional recognition process and the execution of rescue-like behavior.

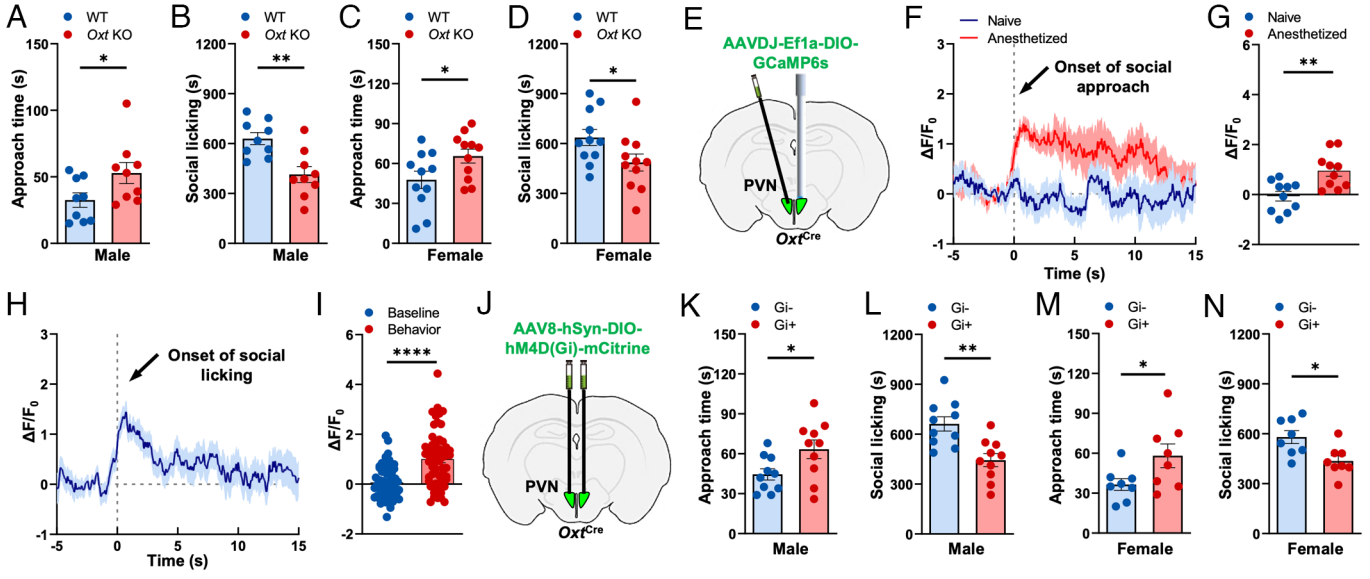

Fig. 2. OXT^{PVN} signaling mediates rescue-like behavior. (*A*–*D*) Approach (*A* and *C*) and social licking time (*B* and *D*) for WT and *Oxt* KO observers (n = 9 for each male group, n = 11 for each female group). (*E*) Schematic of fiber photometry recording of PVN^{OXT} neurons. (*F* and *G*) Averaged trace (*F*) and mean $\Delta F/F_0$ (*G*) of OXT^{PVN} Ca^{2+} signals during the social approach to anesthetized or naïve mouse (n = 10 trials for each group). (*H* and *I*) Averaged trace (*H*) and mean $\Delta F/F_0$ (*I*) of OXT^{PVN} Ca^{2+} signals perionset of social licking (n = 57 trials). (*J*) Schematic of PVN virus injection in the Oxt^{Cre} mice for chemogenetic inhibition. (*K*–*N*) Approach (*K* and *M*) and social licking time (*L* and *N*) for Gi– and Gi+ observers (n = 10 for each male group, n = 8 for each female group). Statistical analyses included paired-sample *t* test (*G*), independent-sample *t* test (*A*–*D*, *I*, and *K*–*N*). **P* < 0.05, ***P* < 0.01, *****P* < 0.0001. Data are means ± SEM. OXT, oxytocin; PVN, paraventricular nucleus of the hypothalamus.

The OXT^{PVN}-$OXTR^{CeA}$ Projection Pathway Regulates Emotional Process. PVN^{OXT} neurons send efferent projections to multiple brain regions, including the central nucleus of the amygdala (CeA) (46–48), a key hub involved in social function (40). In particular, the oxytocin receptor (OXTR)-expressing neurons in the CeA ($OXTR^{CeA}$) are associated with recognizing the emotional states of conspecifics (40). To investigate this pathway, we first examined monosynaptic connections between OXT^{PVN} and $OXTR^{CeA}$ neurons using a rabies retrovirus tracing approach in $Oxtr^{Cre}$ mice (*SI Appendix*, Fig. S3 *A–C*). This analysis showed enriched Cre expression in the CeA (*SI Appendix*, Fig. S3 *D–G*), consistent with previous findings (49). We then monitored the neural dynamics of $OXTR^{CeA}$ neurons during social approach and social licking by measuring Ca^{2+} transients using fiber photometry in $OXTR^{CeA}$ neurons expressing AAVDJ-Ef1a-DIO-GCaMP6s (Fig. 3*A* and *SI Appendix*, Fig. S4*A*). Notably, Ca^{2+} activity gradually increased as the observer mouse approached the anesthetized demonstrator (Fig. 3 *B* and *C* and *SI Appendix*, Fig. S4*B*) and exhibited a rapid surge at the onset of social licking (Fig. 3 *D* and *E*, *SI Appendix*, Fig. S4*C*, and Movie S3). These results suggest that $OXTR^{CeA}$ neurons are involved in emotional recognition and rescue-like behavior.

To further assess the function of $OXTR^{CeA}$ neurons, we used optogenetics to selectively inhibit their activity by expressing either a control virus (AAV5-Ef1a-DIO-eYFP) or AAV5-CAG-FLEX-Jaws-GFP virus in the CeA of $Oxtr^{Cre}$ mice (Fig. 3*F* and *SI Appendix*, Fig. S4*D*). Opto-inhibition prolonged approach behavior while reducing social licking time (Fig. 3 *G* and *H*). To selectively inhibit the PVN-CeA OXT neuronal projection ($OXT^{PVN\text{-}CeA}$), we expressed AAV5-Ef1a-DIO-eYFP (control group) or AAV5-CAG-FLEX-Jaws-GFP virus in the PVN and implanted optic fibers into the CeA of Oxt^{Cre} mice (Fig. 3*I* and *SI Appendix*, Fig. S4*E*). Opto-inhibition of $OXT^{PVN\text{-}CeA}$ neuronal projection similarly delayed approach behavior while reducing social licking time (Fig. 3 *J* and *K*). To further assess the valence of the $OXT^{PVN\text{-}CeA}$ neural pathway, we expressed either AAV5-Ef1a-DIO-eYFP (control group) or AAV5-Ef1a-DIO-hChR2-eYFP in the PVN of Oxt^{Cre} mice (*SI Appendix*, Fig. S5 *A* and *B*) and performed the real-time place preference test (RTPP) using optogenetics (*SI Appendix*, Fig. S5*C*). Mice spent significantly less time in the chamber paired with opto-activation of $OXT^{PVN\text{-}CeA}$ neurons (*SI Appendix*, Fig. S5*D*). Together, these results suggest that the OXT^{PVN}-$OXTR^{CeA}$ projection pathway processes the emotion with negative valence and plays a key role in mediating rescue-like behavior.

An OXT^{PVN}-$OXTR^{CeA}$ Peptidergic Pathway Mediates Emotional Function in Rescue-Like Behavior. To determine the role of OXT within the PVN-CeA pathway in rescue-like behavior, we utilized fiber photometry to monitor OXT dynamics in the CeA. We injected an AAV virus expressing fluorescent OXT-sensor (AAV-hSyn-OXT1.0) and implanted an optic fiber into CeA (Fig. 4*A* and *SI Appendix*, Fig. S6*A*). This sensor provides a highly sensitive and temporally precise readout of extracellular OXT fluctuations (50). We found that OXT levels gradually increased and remained elevated when observers approached anesthetized demonstrators, whereas no significant changes occurred during interaction with naïve (nonanesthetized) demonstrators (Fig. 4 *B* and *C* and *SI Appendix*, Fig. S6*B*). Additionally, OXT levels exhibited a rapid surge at the onset of social licking, followed by a gradual decline (Fig. 4 *D* and *E* and *SI Appendix*, Fig. S6*C*). These findings suggest that OXT release into the CeA is selectively triggered by social cues from anesthetized mice, potentially driving rescue-like behavior.

To examine whether $OXTR^{CeA}$ neurons that receive PVN efferents exert a functional role in rescue-like behavior, we designed a viral-mediated strategy, injecting AAV1-Ef1a-IRES-Flpo virus into the PVN and Flpo-dependent virus (AAV8-Ef1a-fDIO-Cre-mCherry) into the CeA of $Oxtr^{f/f}$ mice, respectively (Fig. 4*F*). This strategy allowed Flpo recombinase to be transported anterogradely into the CeA of $Oxtr^{f/f}$ mice, selectively deleting *Oxtr* in neurons directly innervated by PVN neurons (*SI Appendix*, Fig. S6*D*). The

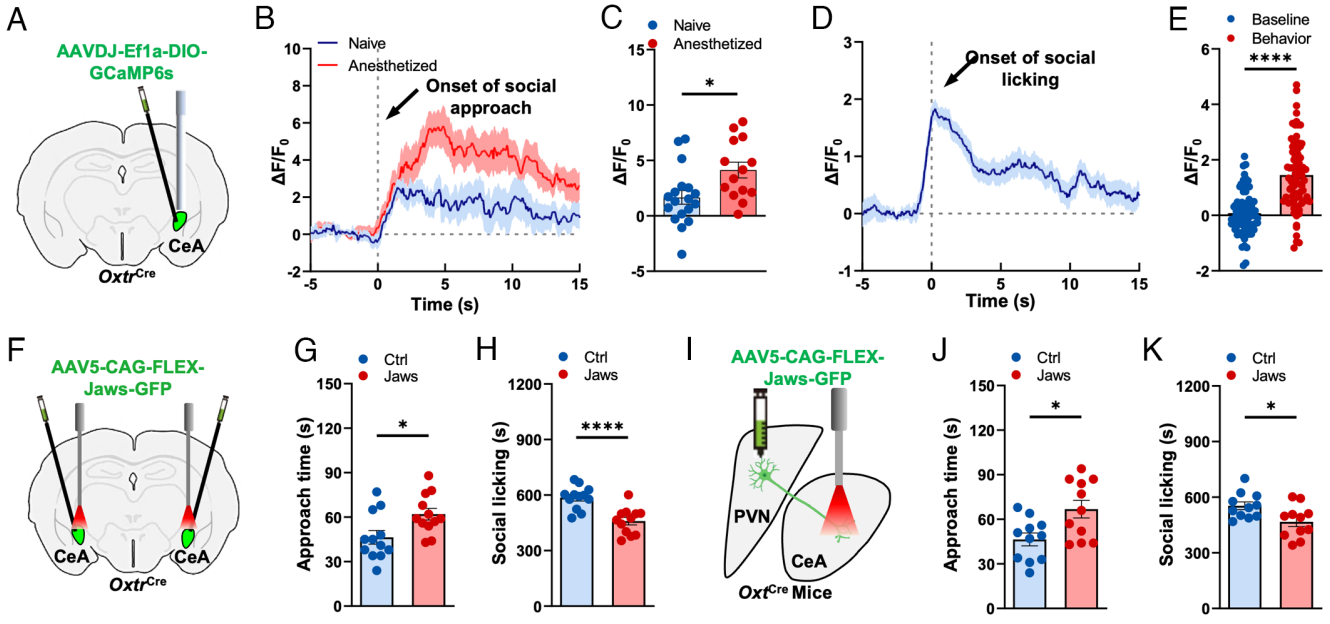

Fig. 3. OXT^{PVN}-$OXTR^{CeA}$ projection regulates the emotional process of rescue-like behavior. (*A*) Schematic of fiber photometry recording of $OXTR^{CeA}$ neurons. (*B* and *C*) Averaged trace (*B*) and mean $\Delta F/F_0$ (*C*) of $OXTR^{CeA}$ Ca^{2+} signals during the social approach to anesthetized or naïve mouse (n = 18 trials for naïve, n = 14 for the anesthetized). (*D* and *E*) Averaged trace (*D*) and mean $\Delta F/F_0$ (*E*) of $OXTR^{CeA}$ Ca^{2+} signals perionset of social licking (n = 75 trials). (*F*) Schematic of optogenetic inhibition of $OXTR^{CeA}$ neurons. (*G* and *H*) Approach (*G*) and social licking time (*H*) with long-term optogenetic inhibition of $OXTR^{CeA}$ Jaws or control (n = 6 males + 6 females for each group). (*I*) Schematic of optogenetic inhibition of OXT^{PVN} efferents in CeA. (*J* and *K*) Approach (*J*) and social licking time (*K*) with long-term optogenetic inhibition of $PVN^{OXT\text{-}CeA}$ Jaws or control (n = 6 males + 5 females for each group). Statistical analyses included paired-sample *t* test (*E*) and independent-sample *t* test (*C*, *G*, *H*, *J*, and *K*). $*P < 0.05$, $****P < 0.0001$. Data are means ± SEM. CeA, central nucleus of the amygdala.

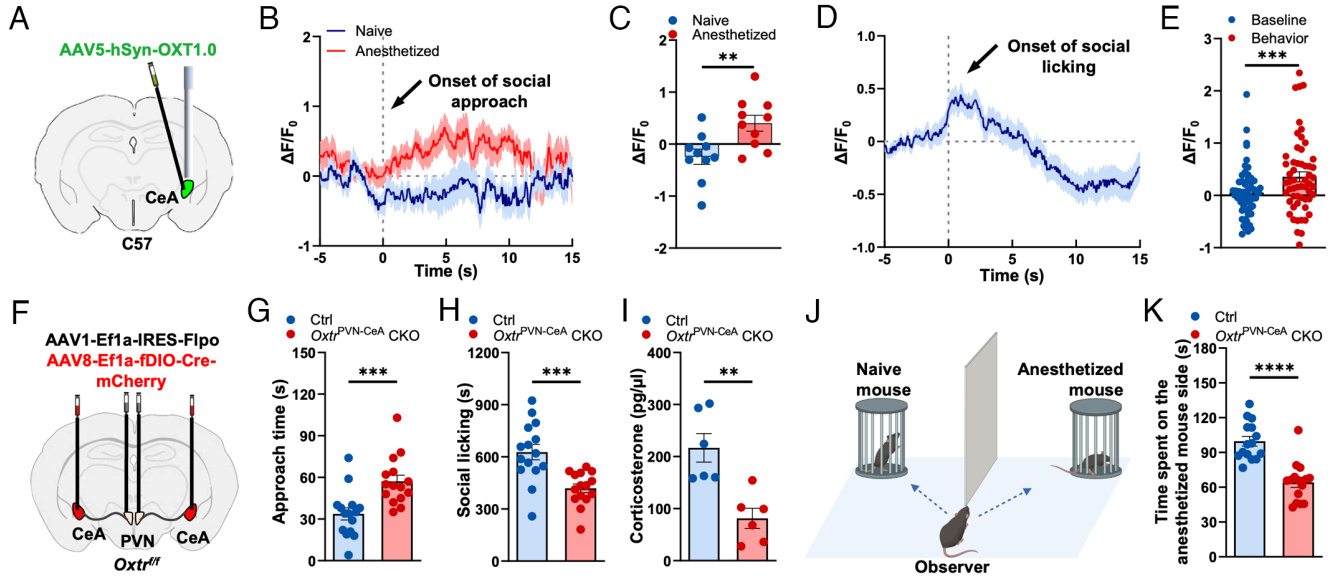

Fig. 4. The OXT^{PVN}-OXTR^{CeA} peptidergic pathway mediates stress-related emotional function in rescue-like behavior. (*A*) Schematic of fiber photometry recording of OXT-sensor. (*B* and *C*) Averaged trace (*B*) and mean $\Delta F/F_0$ (*C*) of OXT-sensor in CeA during the social approach to the anesthetized or naïve mouse (n = 10 trials for each group). (*D* and *E*) Averaged trace (*D*) and mean $\Delta F/F_0$ (*E*) of OXT-sensor in CeA perionset of social licking (n = 56 trials). (*F*) Schematic of virus injection into the PVN and CeA of *Oxtr*$^{f/f}$ mice. (*G* and *H*) Approach (*G*) and social licking time (*H*) for control or *Oxtr*$^{PVN\text{-}CeA}$ CKO mice (n = 8 males + 7 females for each group). (*I*) Plasma corticosterone level at 20 min of rescue-like behavior test for control or *Oxtr*$^{PVN\text{-}CeA}$ CKO mice (n = 6 males for each group). (*J* and *K*) Emotional discrimination test schematic (*J*) and time on the anesthetized mouse side for control or *Oxtr*$^{PVN\text{-}CeA}$ CKO mice (*K*) (n = 8 males + 7 females for each group). Statistical analyses included paired-sample *t* test (*E*) and independent-sample *t* test (*B*, *G–I*, and *K*). $^{**}P < 0.01$, $^{***}P < 0.001$, $^{****}P < 0.0001$; ns, no significance. Data are means ± SEM.

resulting mice were thereafter referred to as *Oxtr*$^{PVN\text{-}CeA}$ CKO mice. Consistent with our hypothesis, these CKO mice prolonged approach time, reduced licking behavior (Fig. 4 *G* and *H*), and had lower CORT levels (Fig. 4*I*). Furthermore, in an emotional discrimination test, the CKO mice spent significantly less time interacting with anesthetized demonstrators (Fig. 4 *J* and *K*). Together, these results demonstrate that OXT^{PVN}-OXTR^{CeA} signaling is crucial for recognizing anesthetized conspecifics, processing emotional stress, and driving rescue-like behavior.

The OXT^{PVN}-OXTR^{dBNST} Pathway Controls the Motor Function of Licking Behavior but Not Emotional Valence. OXTR^{+} neurons in the BNST play a crucial role in various social behaviors (51–54) and receive direct input from the PVN^{OXT} neurons (*SI Appendix*, Fig. S7) (46, 55). To ascertain whether BNST OXTR^{+} neurons contribute to rescue-like behavior, we monitored Ca^{2+} dynamics using fiber photometry after expressing AAVDJ-DIO-GCaMP6s in the dorsal or ventral BNST (referred to as the OXTR^{dBNST} and OXTR^{vBNST}, respectively) of *Oxtr*^{Cre} mice (Fig. 5*A* and *SI Appendix*, Figs. S8*A* and S9*A*). During social interaction, although the Ca^{2+} signal increased (Fig. 5*B* and *SI Appendix*, Fig. S9*B*), we did not detect significant differences between approaching anesthetized and naïve demonstrators (Fig. 5*C*). However, we observed a rapid and pronounced increase in Ca^{2+} signal in dBNST neurons (Fig. 5 *B* and *C*, *SI Appendix*, Fig. S9*C*, and Movie S4), but not in vBNST neurons, coinciding with the onset of social licking (*SI Appendix*, Fig. S8 *B–D*). These findings indicate that OXTR^{dBNST} neurons contribute to rescue-like behavior but are not involved in emotional discrimination.

Next, we optogenetically activated or inhibited OXTR^{dBNST} neurons by expressing AAV5-Ef1a-DIO-hChR2-eYFP, AAV5-CAG-FLEX-Jaws-GFP, or AAV5-Ef1a-DIO-eYFP (control group) virus in the dBNST of *Oxtr*^{Cre} mice (Fig. 5 *F* and *J* and *SI Appendix*, Fig. S9 *D* and *E*), respectively. Opto-activation of OXTR^{dBNST} neurons substantially increased social licking behavior (Fig. 5*G* and Movie S5). In the absence of demonstrators, opto-activation still elicited robust licking behavior directed at the chamber wall (Fig. 5*H* and Movie S6) without affecting self-grooming behavior (Fig. 5*I*). Conversely, real-time opto-inhibition of OXTR^{dBNST} neurons profoundly disrupted social licking behavior toward demonstrators (Fig. 5*K* and Movie S7). These results indicate that OXTR^{dBNST} neurons regulate the motor execution of licking behavior but do not participate in emotional recognition.

Next, we explored the PVN-dBNST projection pathway by expressing AAV5-Ef1a-DIO-hChR2-eYFP, AAV5-CAG-FLEX-Jaws-GFP, or AAV5-Ef1a-DIO-eYFP (control group) virus in the PVN and implanting optic fibers into the dBNST of *Oxt*^{Cre} mice (Fig. 5 *L* and *P* and *SI Appendix*, Fig. S9 *F* and *G*). This allows selective activation or inhibition of dBNST-projecting efferents of OXT^{PVN} neurons, hereafter referred to as the OXT$^{PVN\text{-}dBNST}$. Consistently, opto-activation increased social licking (Fig. 5*M*), whereas opto-inhibition disrupted it (Fig. 5*Q*). Additionally, the RTPP test showed that opto-activation of the OXT$^{PVN\text{-}dBNST}$ pathway did not induce preference or avoidance behavior (Fig. 5 *N* and *O*), suggesting that this pathway mediates licking behavior but does not encode emotional valence.

The OXT^{PVN}-OXTR^{dBNST} Peptidergic Pathway Is Required for Licking Behavior. To examine the OXT release from the PVN into the dBNST during rescue-like behavior, we employed fiber photometry to monitor OXT-sensor fluorescence within the dBNST (Fig. 6*A* and *SI Appendix*, Fig. S10*A*). A rapid increase in OXT levels was observed at the onset of social licking (Fig. 6 *D* and *E* and *SI Appendix*, Fig. S10*C*), whereas no significant changes occurred during the social approach to either anesthetized or naïve conspecifics (Fig. 6 *B* and *C* and *SI Appendix*, Fig. S10*B*). Next, we selectively deleted *Oxtr* in dBNST neurons receiving PVN projections (referred to as *Oxtr*$^{PVN\text{-}dBNST}$ CKO) using a virus-mediated strategy. Specifically, we injected an anterogradely transported virus (AAV1-Ef1a-IRES-Flpo) into the PVN and Flpo-dependent virus (AAV8-Ef1a-fDIO-Cre-mCherry) into the dBNST of *Oxtr*$^{f/f}$ mice (Fig. 6*F* and *SI Appendix*, Fig. S10*D*), generating *Oxtr*$^{PVN\text{-}dBNST}$ CKO mice. Behaviorally, *Oxtr*$^{PVN\text{-}dBNST}$

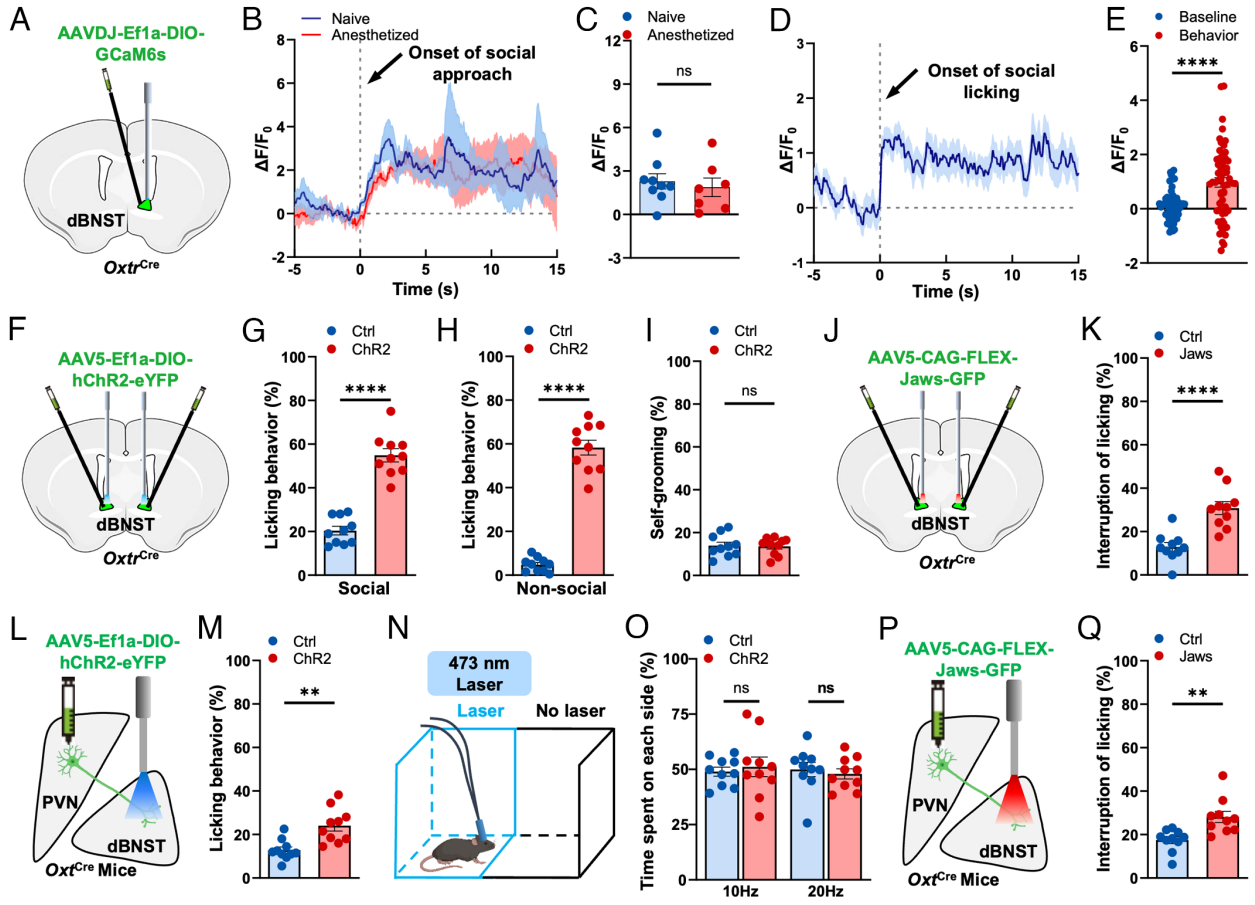

Fig. 5. OXT^{PVN}-OXTR^{dBNST} projection regulates licking-related motor function in rescue-like behavior. (*A*) Schematic of fiber photometry recording of OXTR^{dBNST} neurons. (*B* and *C*) Averaged trace (*B*) and mean $\Delta F/F_0$ (*C*) of OXTR^{dBNST} Ca^{2+} signals during the social approach to the anesthetized or naïve mouse (n = 9 trials for naïve, n = 7 for anesthetized). (*D* and *E*) Averaged trace (*D*) and mean $\Delta F/F_0$ (*E*) of OXTR^{dBNST} Ca^{2+} signals perionset of social licking (n = 58 trials). (*F*) Schematic of optogenetic activation of OXTR^{dBNST} neurons. (*G* and *H*) Licking behavior ratio in social (*G*) or nonsocial (*H*) context with activation of OXTR^{dBNST} ChR2 or control (n = 5 males + 5 females for each group). (*I*) Self-grooming ratio with activation onset in OXTR^{dBNST} ChR2 or control (n = 5 males + 5 females for each group). (*J*) Schematic of optogenetic inhibition of OXTR^{dBNST} neurons. (*K*) Interruption ratio of licking/grooming behavior with real-time inhibition of OXTR^{dBNST} Jaws or control (n = 5 males + 5 females for each group). (*L*) Schematic of optogenetic activation of OXT^{PVN} efferents in dBNST. (*M*) Licking behavior ratio with activation of OXT$^{PVN\text{-}dBNST}$ ChR2 or control (n = 6 males + 4 females for each group). (*N* and *O*) Schematic (*N*) and behavioral results (*O*) of RTPP test for OXT$^{PVN\text{-}dBNST}$ ChR2 or control mice (n = 6 males + 4 females for each group). (*P*) Schematic of optogenetic inhibition of OXT^{PVN} efferents in dBNST. (*Q*) Interruption ratio of licking/grooming behavior with inhibition of OXT$^{PVN\text{-}dBNST}$ Jaws or control (n = 6 males + 4 females for each group). Statistical analyses included paired-sample *t* test (*E*), independent-sample *t* test (*C*, *G–I*, *K*, *M*, and *Q*), and two-way ANOVA with Tukey's multiple comparison (*O*). $^{**}P < 0.01$, $^{****}P < 0.0001$; ns, no significance. Data are means ± SEM. dBNST, dorsal bed nucleus of the stria terminalis. RTPP, real-time place preference.

CKO mice showed significant impairments in social licking (Fig. 6*H*) without alterations in approach behavior (Fig. 6*G*). Furthermore, these mice retained their ability to recognize anesthetized conspecifics (Fig. 6 *I* and *J*). Collectively, these findings indicate that the OXT^{PVN}-OXTR^{dBNST} signaling is not involved in emotional processing but plays a specific role in the execution of rescue-like behavior.

OXT^{PVN}-OXTR^{CeA} and OXT^{PVN}-OXTR^{dBNST} Signaling Pathways Display Distinct Responding Patterns. To further elucidate the functional differences between PVN-CeA and PVN-dBNST pathways, we evaluate the potential causal relationship between fiber photometry data and social licking behavior duration (56). First, we quantified the signal intensity (defined by peak height) and signal duration (defined by signal width) from fluorescence recordings of individual trials. We then analyzed single-trial correlations between peak height and social licking time and between signal width and social licking time (Fig. 7*A* and *SI Appendix*, Fig. S11).

Our analysis revealed that in the dBNST, signal width (Fig. 7 *B* and *D*), but not peak height (Fig. 7 *C* and *E*), correlated with behavior time (i.e., social licking duration). In contrast, in the CeA, peak height (Fig. 7 *G* and *I*), but not signal width (Fig. 7 *F* and *H*), correlated with behavior time. Additionally, CeA signals predominantly peaked at the onset of social licking behavior, occurring within the first 5 s (*SI Appendix*, Fig. S12 *C* and *D*), suggesting that the OXT^{PVN}-OXTR^{CeA} signal pathway acts as an initiator rather than a maintainer of licking behavior. Notably, both the signal width and peak height of OXT^{PVN} neurons correlated with behavior time (*SI Appendix*, Fig. S12 *A* and *B*), indicating that the dynamics of OXT^{PVN} neurons incorporate both response patterns, serving as the shared upstream modulator of the two pathways. In summary, these findings reveal that the OXT^{PVN}-OXTR^{dBNST} pathway exhibits a sustained response pattern, aligning with the duration of social licking behavior, whereas the OXT^{PVN}-OXTR^{CeA} operates transiently and intensely, acting as a trigger for social licking behavior (Fig. 7*J*).

Discussion

This study demonstrates that mice can innately perform rescue-like behavior, accelerating the recovery of anesthetized conspecifics from an unconscious state. While previous studies have reported rescue-like behaviors in rodents (28), these behaviors were acquired through

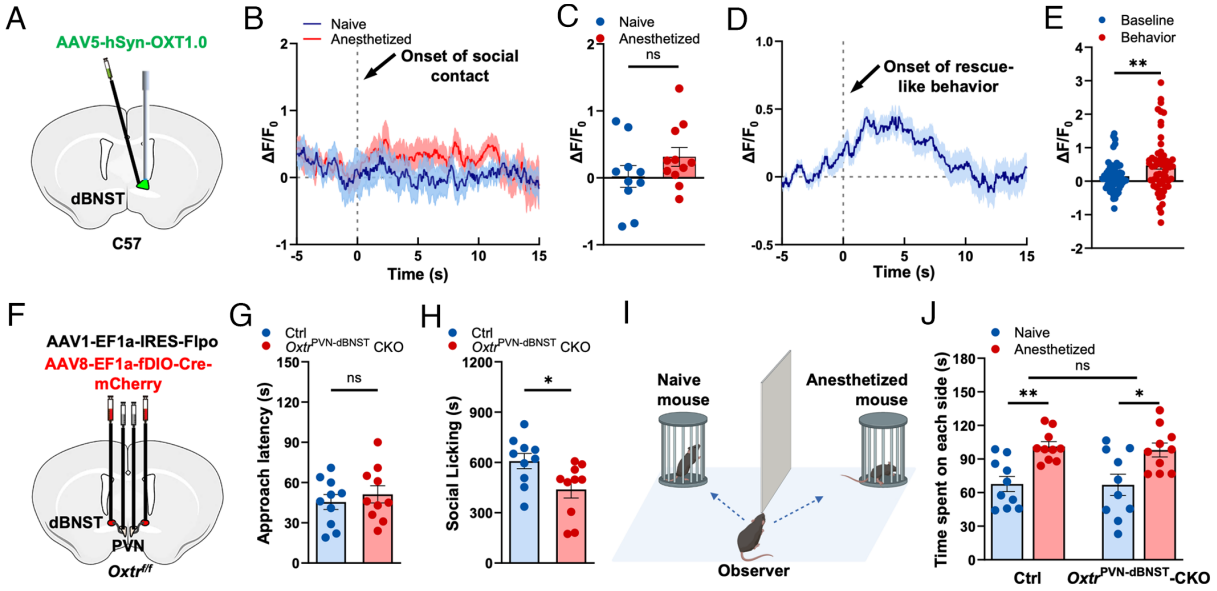

Fig. 6. OXT^{PVN}-OXTR^{dBNST} peptidergic pathway mediates motor but not emotional function in rescue-like behavior. (*A*) Schematic of fiber photometry recording of OXT-sensor. (*B* and *C*) Averaged trace (*B*) and mean $\Delta F/F_0$ (*C*) of OXT-sensor in dBNST during the social approach to the anesthetized or naïve mouse (n = 10 trials for each group). (*D* and *E*) Averaged trace (*D*) and mean $\Delta F/F_0$ (*E*) of OXT-sensor in dBNST perionset of social licking (n = 36 trials). (*F*) Schematic of virus injection into the PVN and dBNST of *Oxtr*$^{f/f}$ mice. (*G* and *H*) Approach (*G*) and social licking time (*H*) for control or *Oxtr*$^{PVN\text{-}dBNST}$ CKO mice (n = 5 males + 5 females for each group). (*I* and *J*) emotional discrimination test schematic (*I*) and time spent (*J*) on the naïve or anesthetized mouse side for control or *Oxtr*$^{PVN\text{-}dBNST}$ CKO mice (n = 5 males + 5 females for each group). Statistical analyses included paired-sample *t* test (*E*), independent-sample *t* test (*C*, *G*, and *H*), and two-way ANOVA with Tukey's multiple comparison (*J*). $^*P < 0.05$, $^{**}P < 0.01$; ns, no significance. Data are means ± SEM.

learning rather than being instinctual. In contrast, the rescue-like behavior identified here occurs spontaneously, making it a valuable model for investigating its underlying mechanisms. Notably, we show that social licking behavior facilitates earlier emergence from unconsciousness while reducing distress in helper mice. The spontaneous nature of this behavior—occurring without prior social experience of anesthetized conspecifics, learning processes, external apparatus, or explicit rewards—reveals a broader and more sophisticated capacity for helping behavior in rodents than previously recognized. Our findings expand our understanding of rodent prosociality and establish a framework for studying the neural and molecular mechanisms underlying this essential behavior in laboratory settings.

During the revision of this study, three independent teams reported rescue-like behaviors in mice (57–59), mainly aligning with our findings. However, several differences exist between our results and theirs. First, both our study and the study of of Sun et al. (58) identified social grooming and licking as the predominant behaviors, whereas Cao et al. (57) and Sun et al. (59) primarily observed biting and tongue-dragging as the primary helping behavior. Second, consistent with our findings, two studies indicated that mice predominantly exhibit rescue or helping behaviors toward living rather than deceased partners (57, 58). In contrast, the third group reported reviving-like behaviors directed at both unconscious and dead conspecifics (59). Additionally, our study analyzed an entire 60-min behavioral session, whereas the other three studies focused mainly on the first 15 to 20 min. This broader observation window may provide deeper insights into the dynamics of these behaviors. Furthermore, our study uniquely differentiates the molecular and neural pathways underlying the emotional and motor components of rescue-like actions. While some of these differences may be attributed to technical reasons, all four studies provide compelling evidence for the existence of spontaneous rescue-like behavior in mice, laying the groundwork for future investigation into its underlying mechanisms.

Social grooming and licking involve a series of complex and stereotypic processes, including emotion recognition, approach, interaction, and targeted helping behavior. As an important form of prosocial behavior, these actions play a crucial role in strengthening social bonds and improving the well-being of social animals (17, 60–62). Such helping behaviors may also contribute to the demonstrator's recovery, rather than serving merely as exploratory or playful actions (18, 63). The observation that mice predominantly engage in social licking toward anesthetized or comatose demonstrators—rather than dead or fake mice—suggests goal-directed helping behavior is only meaningful when the intended outcome might be achievable. Future studies are needed to examine the underlying molecular and neural mechanisms driving this rescue-like behavior, i.e., from perception to action (64). Additionally, how social licking or grooming facilitates the recovery of anesthetized conspecifics remains an intriguing question for further research.

We identified subcortical peptidergic pathways mediating rescue-like behavior's emotional and motor components by adopting this behavioral paradigm and employing interdisciplinary approaches. Specifically, we show that OXT release from PVN neurons targets OXTR in the CeA and dBNST, regulating distinct aspects of this behavior. The OXT^{PVN}-OXTR^{CeA} pathway mediates stress-related negative emotions induced by interactions with anesthetized conspecifics, triggering rescue-like behavior. This finding underscores the critical role of CeA in processing emotional valence (65, 66) and exerting anxiolytic effects (46, 47). On the other hand, our findings reveal that the OXT^{PVN}-OXTR^{dBNST} pathway governs motor functions rather than stress or anxiety regulation (67). Together, these findings illustrate the intricate specificity of subcortical OXT signaling, demonstrating its distinct functional roles in modulating different facets of rescue-like behavior. By elucidating these mechanisms, our data support that targeted helping behavior is genetically programmed, with some underlying processes evolutionarily conserved across the animal kingdom (6, 8, 12).

This study integrates Ca^{2+} and OXT signaling to investigate molecular and neuronal activities during prosocial behavior. Our

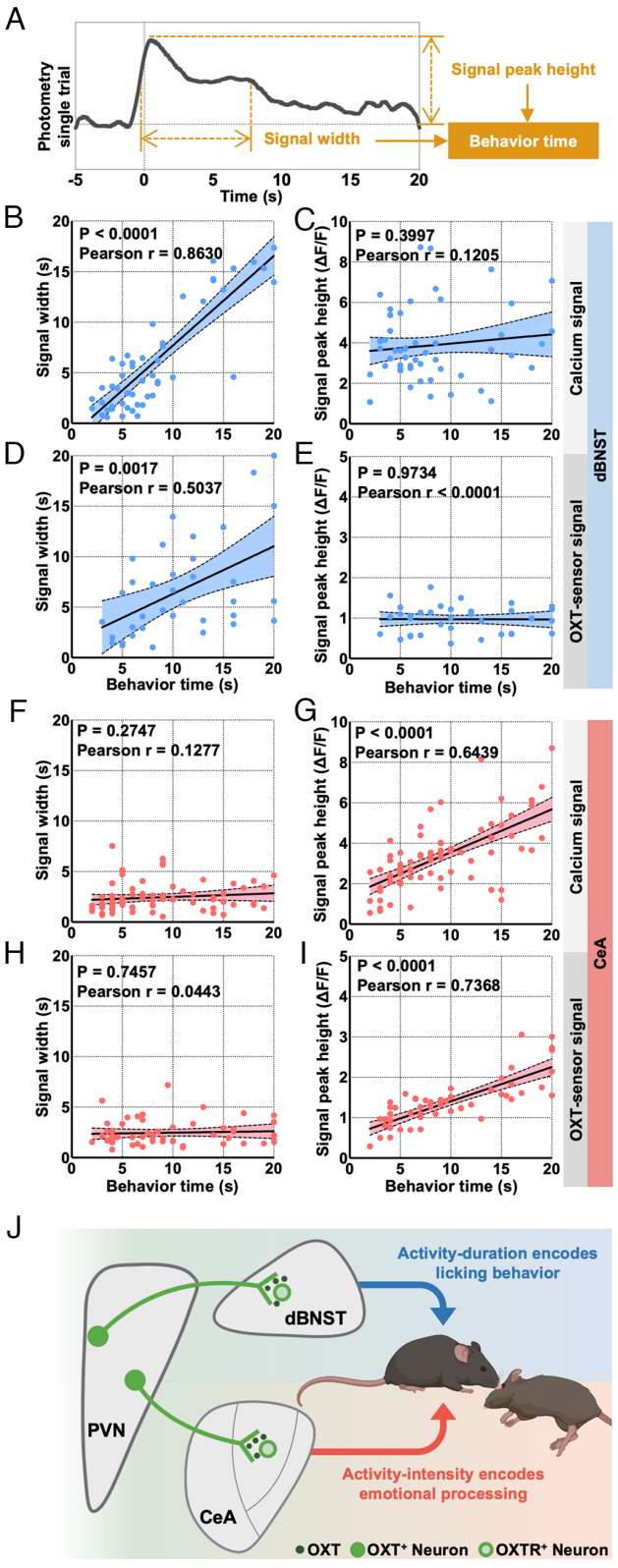

Fig. 7. $OXT^{PVN\text{-}CeA}$ and $OXT^{PVN\text{-}dBNST}$ signaling pathways display distinct activity patterns during rescue-like behavior. (*A*) An example trace showing photometry recorded signal width and peak height in relation to the rescue-like behavior time in one licking/grooming bout. (*B* and *C*) The linear regression of $OXTR^{dBNST}$ $Ca2^{+}$ signal width (*B*) and peak height (*C*) with the behavior time. (*D* and *E*) The linear regression of dBNST OXT-sensor signal width (*D*) and peak height (*E*) with the behavior time. (*F* and *G*) The linear regression of $OXTR^{CeA}$ $Ca2^{+}$ signal width (*F*) and peak height (*G*) with the behavior time. (*H* and *I*) The linear regression of CeA OXT-sensor signal width (*H*) and peak height (*I*) with the behavior time. (*J*) Schematic depicting distinct subcortical OXT signaling pathways that independently control motor function of licking behavior and emotion component of rescue-like behavior. Statistical analyses used Pearson r correlation in *B*–*I*.

findings reveal distinct spatiotemporal dynamics and response patterns of Ca^{2+} and OXT signals within two separate pathways (*SI Appendix*, Fig. S12*E*). Specifically, in the CeA, signal intensity correlates with behavioral timing, whereas in the dBNST, the signal duration exhibits a correlation. In the CeA, the transient increase at the onset of behavior suggests a role in affective salience coding, which is necessary for triggering rescue-like behavior. In contrast, activation of the OXT^{PVN}-$OXTR^{dBNST}$ pathway follows a sustained pattern synchronized with the duration of rescue-like behavior, providing strong evidence that this pathway governs and maintains the motor function of licking behavior.

In conclusion, our study reveals rodents' remarkable and unexpected capacity to adapt their behavior to assist anesthetized conspecifics in potential danger. We provide evidence for the involvement of two parallel subcortical OXT-OXTR signaling pathways, which operate independently yet synergistically to regulate social approach, initiation, and continuation of spontaneous rescue-like behavior. The automatic activation of these pathways by salient social cues suggests that targeted helping behavior is driven by a more primitive bottom–up control process. These findings, together with the highly conserved role of OXT signaling in facilitating prosocial behavior and the presence of ancestral hypothalamus–limbic circuits, offer further support for the evolutionarily conserved molecular and neural mechanisms underlying emotional contagion, empathy, and prosocial behavior across rodents and humans.

Limitations of the Study. This study reveals distinct functions of subcortical OXT-OXTR signaling in these two processes. However, several key questions remain unanswered. It is still unclear how observer mice infer the affective state of anesthetized conspecifics and experience distress and the precise nature of sensory cues (e.g., visual and/or olfactory) emitted by anesthetized individuals. Additionally, how these sensory inputs are integrated at the PVN level and subsequently translated into targeted motor output and motivational drive underlying rescue behavior remains unknown. Given the heterogeneity of OXT^{PVN} neurons and the absence of genetic markers for their subtypes (68), we cannot yet determine whether distinct populations of OXT neurons separately mediate emotional valence processing and licking behavior. Future studies are needed to elucidate the sensory input pathways and emotional and motor output circuits that act in concert to orchestrate motivated helping behavior.

Methods

Mice. 12- to 28-wk-old mice were used for all experiments except the 2-mo and 9-mo groups. Ages from 7 to 8 wk were used as 2-mo subjects, and ages from 8 to 9 mo were used as old subjects (69). All experiments were performed in accordance with the guidelines of the NIH and the International Association for the Study of Pain and were approved by the Animal Studies Committee at both Washington University School of Medicine and Shenzhen Bay Laboratory.

Experimental Design for Rescue-Like Behavior Paradigm. Before the behavior test, an observer was placed into a testing chamber (15 × 15 × 15 cm) to acclimate for 60 min. During the acclimation, food (2 to 3 g) and water (2 to 3 g hydrogel) were placed in the chamber. After the acclimation, a demonstrator was administered an intraperitoneal injection (i.p.) of a ketamine cocktail (ketamine: 10 mg/mL + xylazine: 1 mg/mL, 10 μL/g body weight) for anesthesia model, high dose of clozapine (1 mg/g body weight) for comatose model, or 10% chloral hydrate (4 μL g body weight) for deep sedation model. 3 to 5 min later, the demonstrator exhibited the LORR. Subsequently, the demonstrator was placed in the testing chamber for video recording. A total of 60-min video recording was conducted. Dead demonstrators were utilized for experiments 5 min or 4 h after death, with their appearance and fur remaining intact. For cagemate

experiments, observers and demonstrators were littermates and housed in the same cage (14). For stranger experiments, observers and demonstrators were raised in different cages.

Videos from all experiments were viewed by raters blinded to the treatments and mouse genotypes. Body grooming and facial licking behaviors were identified from the videos and analyzed as rescue-like behavior. Body grooming was defined as the observer's head contact with the demonstrator's body, accompanied by rhythmic head movements (17). Facial licking was defined as the observer's tongue or mouth licking the demonstrator's eyes, cheek, or mouth. The duration of the licking/ grooming behavior (referred to as the social licking time) and the timepoint of the first behavior episode (referred to as the approach time) were used for analyses.

Experimental Design for Divider Paradigm. The observer was acclimated in the testing chamber (15 × 15 × 15 cm) for 60 min. After the acclimation, the demonstrator received i.p. of saline or ketamine cocktail. A divider was set in the middle of the testing chamber, dividing the chamber into two equal zones, and the observer and demonstrator were put into different zones.

After 20, 40, and 60 min, we quietly removed the demonstrator from the testing chamber and released 5% isoflurane into the testing chamber to quickly anesthetize the observer. Then 400 μL blood was collected into lithium heparin tubes by submandibular bleeding for ELISA.

Plasma Collection and ELISA Assay. Blood was centrifuged at 10,000 rpm for 5 min at 4 °C. Then the supernatant was collected and stored at −80 °C until the assay. CORT concentrations were detected from mice plasma by ELISA kits following the manufacturer's protocols. The optical density of CORT was analyzed by CurveExpert 1.4.

Emotional Discrimination Test. The test was performed as previously described (40). Briefly, we first put a naive and an anesthetized demonstrator into two wire cups, respectively. Then we put the observer in the middle of the testing chamber and started video recording for 6 min. The observer was unfamiliar with both the anesthetized and naïve animals. ANYMAZE 10 was used to analyze the time spent on the naïve and anesthetized demonstrator sides, which tracks the time the observer spends within a 10 to 12-cm proximity to the demonstrator.

Immunohistochemistry (IHC) and RNAscope. IHC was performed as previously described (70). RNAscope ISH was performed according to our previous studies (71).

Chemogenetic Inhibition. For DREADD (Designer Receptors Exclusively Activated by Designer Drugs) experiments, clozapine is used in the chemogenetic test (72). Before the test, an observer was injected with clozapine (0.1 μg/g weight, i.p.) and then acclimated in a testing chamber for 30 min. After the acclimation, an anesthetized demonstrator was put into the testing chamber. The entire 60 min behavior between the observer and demonstrator was recorded by camera.

Optogenetic Manipulations. Prior to test, the observer was connected to a laser system and acclimated in the testing chamber for 60 min, followed by video recording. An Arduino microcontroller controlled the laser.

For the optogenetic activation of $OXTR^{dBNST}$ neurons, $OXT^{PVN-CeA}$ efferent, or $OXT^{PVN-dBNST}$ efferent experiments, 10 ms, 473 nm, 5 to 7 mW/mm^2 laser pulses at 10 Hz were used (16). Laser trains lasted 20 s with 180 s intervals (73). Social context tests involved an observer with an anesthetized demonstrator; nonsocial context tests involved only the observer. Licking and grooming behavior ratios were calculated by dividing the time spent on allo-licking and allo-grooming behaviors during the laser-on period by the total duration of the laser-on period.

For the continuous optogenetic inhibition of $OXTR^{CeA}$ neurons or $OXT^{PVN-CeA}$ efferent, a 638 nm, 8 to 10 mW/mm^2 laser was delivered with 8-s-on and 2-s-off cycles (total 60 min) to the observer (34).

For real-time optogenetic inhibition of $OXTR^{dBNST}$ neurons or $OXT^{PVN-dBNST}$ efferent, a 638 nm, 8 to 10 mW/mm^2 laser was manually delivered when the observer exhibited rescue-like behavior. The laser lasted for 10 to 20 s. The interruption ratio was calculated as the percentage of successful behavior interruptions per total laser trial.

RTPP. RTPP was performed as previously described (74). A two-compartment conditioning apparatus (70 × 35 × 30 cm) was randomly assigned with or without laser stimulation. Mice were connected to a 473 nm laser and acclimated for 3 to 5 min before test. The RTPP test used 10 or 20 Hz photostimulation (10 ms pulse, ~10 mW/mm^2 power) for 15 min, with time spent in each compartment recorded via camera and analyzed with ANYMAZE 10. The place preference ratio was defined as the percentage of time spent on the stimulation-paired side.

Identification of PVN^{OXT} to CeA^{OXTR} and PVN^{OXT} to $dBNST^{OXTR}$ Circuitry. To identify direct innervations of OXT^{PVN} neurons onto $OXTR^{CeA}$ or $OXTR^{dBNST}$ neurons, rabies virus (RV)–dependent monosynaptic retrograde tracing was used (75). *Oxtr*^{Cre} mice received unilaterally injection of 300 nL AAV9-Ef1α-DIO-RVG + AAV9-Ef1α-DIO-His-EGFP-2A-TVA (1:1 volume ratio) into CeA or dBNST. Three weeks later, RV-ENVA-ΔG-dsRed (300 nL) was injected at the same coordinates. After 1 wk, mice were perfused, sectioned, and immunostained with an OXT antibody for identification.

Fiber Photometry. Fiber photometry recordings utilized the Doric Neuroscience Studio system. For the rescue-like behavior test, the observer was connected to the photometry system and acclimated in a 20 × 20 × 30 cm chamber for 60 min. Following acclimation, fiber photometry and video recording began, and an anesthetized demonstrator was put in. Behaviors and fluorescence signals were recorded for 60 min. In order to measure the fluorescence during social contact with naïve or anesthetized demonstrator, a discrimination test was employed with naïve or anesthetized demonstrators, recording behaviors and fluorescence for 10 min.

Raw signals were low-pass filtered at 15 Hz and normalized to ΔF/F0 using Doric Neuroscience Studio. Normalized signals were divided into perievent epochs (−5 to 15 s relative to the onset of social licking or approach toward demonstrators. Baseline correction was applied using the median fluorescence during the baseline period (−2 to −1 s relative to event onset).

For data quantification, mean ΔF/F0 values during the baseline (−3 to 0 s) and behavior (0 to 3 s) periods for social licking were compared using paired-sample *t*-tests. In social contact test, mean ΔF/F0 during interactions with anesthetized or naïve mice (0 to 10 s after contact onset) were compared using independent-sample *t*-tests.

Correlation Analyses of Photometry and Behavior Data. For the fiber photometry data of social licking behavior, the peaks of each single trial were extracted by the *findpeaks* function in MATLAB. Then, the peaks with a width less than 50 ms were removed because the actual calcium fluorescence event is usually longer than 50 ms (76). Next, the peak height, width, and peak location (the peak appearance time relative to the onset of social licking behavior) were determined by the first peak with the greatest prominence value. The peak height, width, and location were used to calculate correlation and linear regression with licking duration (56).

EEG Recording. An observer was acclimated in a 20 × 20 × 30 cm chamber for 60 min before EEG recording. Afterward, a demonstrator was connected to the EEG system (CerePlex Direct, 1,000 Hz) and anesthetized before being placed in the chamber. EEG and video recording were then started simultaneously. Control groups had no observer in the chamber, and EEG signals were recorded for 90 min.

Raw EEG data were bandpass filtered (1 to 100 Hz) and notch filtered (59 to 61 Hz). Time-frequency distributions (TFDs) were calculated from the preprocessed EEG and smoothed with a 7.5 s moving median. Delta-band (1 to 4 Hz) and gamma-band (65 to 99 Hz) powers were averaged from the TFD spectra. Empirical CDFs of delta and gamma power from all five mice were calculated and analyzed with an independent-sample Kolmogorov–Smirnov test.

Statistics. Statistical methods are indicated in the figure legend when used. Statistical analyses were performed using Prism 8. Before statistical comparisons, the normality test (Shapiro–Wilk test) was performed on all datasets. Statistical tests used in this study include *t*-tests, Kolmogorov–Smirnov test, Pearson r correlation, one-way ANOVA, and two-way repeated-measures ANOVA followed by Tukey post hoc tests. Equal variance tests (Bartlett's test) were performed for all statistical analyses. Significance levels indicated are as follows: ns, not significant, $*P < 0.05$, $**P < 0.01$, $***P < 0.001$, $****P < 0.0001$.

Data, Materials, and Software Availability. Scripts have been deposited in GitHub (https://github.com/FR-ZH/PhotometryAnalyses) (77). Data are included in the manuscript and/or supporting information.

ACKNOWLEDGMENTS. We thank K.K.Z., L.B.Z., F.G., X.R.Y., Z.Y.T., X.Z., J.G., G.H.H., X.L., and J.C. for the advises and technical support. The project has been supported by the NIH grants R01NS094344 and R01 DA037261–01A1 (Z.–F.C.); Natural Science Foundation of China grants 32441103 (L.H) and Beijing Natural Science Foundation JQ22018 (L.H); and Shenzhen Bay Laboratory Fund 21290071 (Z.–F.C.).

Author affiliations: [a]Center for the Study of Itch and Sensory Disorders, Department of Anesthesiology, Washington University School of Medicine, St. Louis, MO 63110; [b]State Key Laboratory of Cognitive Science and Mental Health, Institute of Psychology, Chinese Academy of Sciences, Beijing 100101, People's Republic of China; [c]Department of Psychology, University of Chinese Academy of Sciences, Beijing 100101, People's Republic of China; [d]Institute of Neurological and Psychiatric Disorders, Shenzhen Bay Laboratory, Shenzhen 518132, People's Republic of China; [e]Shenzhen Medical Academy of Research and Translation, Shenzhen 518132, People's Republic of China; [f]Department of Medicine, Washington University School of Medicine, St. Louis, MO 63110; [g]Department of Psychiatry, Washington University School of Medicine, St. Louis, MO 63110; and [h]Department of Developmental Biology, Washington University School of Medicine, St. Louis, MO 63110

1. E. L. Quarantelli, Images of withdrawal behavior in disasters: Some basic misconceptions. *Soc. Probl.* **8**, 68–79 (1960).
2. T. Kay, L. Keller, L. Lehmann, The evolution of altruism and the serial rediscovery of the role of relatedness. *Proc. Natl. Acad. Sci. U.S.A.* **117**, 28894–28898 (2020).
3. E. Fehr, U. Fischbacher, The nature of human altruism. *Nature* **425**, 785–791 (2003).
4. C. D. Batson, *Altruism in Humans* (Oxford University Press, New York, 2010).
5. M. A. Nowak, K. Sigmund, Evolution of indirect reciprocity. *Nature* **437**, 1291–1298 (2005).
6. F. B. M. de Waal, Putting the altruism back into altruism: The evolution of empathy. *Annu. Rev. Psychol.* **59**, 279–300 (2008).
7. N. Eisenberg, P. A. Miller, The relation of empathy to prosocial and related behaviors. *Psychol. Bull* **101**, 91–119 (1987).
8. J. Decety, I. B. Bartal, F. Uzefovsky, A. Knafo-Noam, Empathy as a driver of prosocial behavior: Highly conserved neurobehavioral mechanisms across species. *Phil. Trans. R. Soc. Lond B Biol. Sci.* **371**, 20150077 (2016).
9. F. B. M. de Waal, S. D. Preston, Mammalian empathy: Behavioral manifestations and neural basis. *Nat. Rev. Neurosci.* **18**, 498–509 (2017).
10. E. L. Quarantelli, Images of withdrawal behavior in disasters: Some basic misconceptions. *Soc. Probl.* **8**, 68–79 (1960).
11. E. Palagi, A. Celeghin, M. Tamietto, P. Winkielman, I. Norscia, The neuroethology of spontaneous mimicry and emotional contagion in human and non-human animals. *Neurosci. Biobehav. Rev.* **111**, 149–165 (2020).
12. J. Panksepp, J. B. Panksepp, Toward a cross-species understanding of empathy. *Trends Neurosci.* **36**, 489–496 (2013).
13. J. E. C. Adriaense, S. E. Koski, L. Huber, C. Lamm, Challenges in the comparative study of empathy and related phenomena in animals. *Neurosci. Biobehav. Rev.* **112**, 62–82 (2020).
14. D. J. Langford *et al.*, Social modulation of pain as evidence for empathy in mice. *Science* **312**, 1967–1970 (2006).
15. M. L. Smith, C. M. Hostetler, M. M. Heinricher, A. E. Ryabinin, Social transfer of pain in mice. *Sci. Adv.* **2**, e1600855 (2016).
16. Y. E. Wu *et al.*, Neural control of affiliative touch in prosocial interaction. *Nature* **599**, 262–267 (2021).
17. J. P. Burkett *et al.*, Oxytocin-dependent consolation behavior in rodents. *Science* **351**, 375–378 (2016).
18. Q. Zeng, W. Shan, H. Zhang, J. Yang, Z. Zuo, Paraventricular thalamic nucleus plays a critical role in consolation and anxious behaviors of familiar observers exposed to surgery mice. *Theranostics* **11**, 3813–3829 (2021).
19. K. L. Hollis, E. Nowbahari, Toward a behavioral ecology of rescue behavior. *Evol. Psychol.* **11**, 647–664 (2013).
20. P. Mason, Lessons from helping behavior in rats. *Curr. Opin. Neurobiol.* **68**, 52–56 (2021).
21. E. R. Vogel, A. Fuentes-Jimenez, Rescue behavior in white-faced capuchin monkeys during an intergroup attack: Support for the infanticide avoidance hypothesis. *Am. J. Primatol.* **68**, 1012–1016 (2006).
22. M. Masilkova *et al.*, Observation of rescue behavior in wild boar (*Sus scrofa*). *Sci. Rep.* **11**, 16217 (2021).
23. R. L. Pitman *et al.*, Humpback whales interfering when mammal-eating killer whales attack other species: Mobbing behavior and interspecific altruism? *Mar. Mammal. Sci.* **33**, 7–58 (2017).
24. M. Hammers, L. Brouwer, Rescue behavior in a social bird: Removal of sticky "bird-catcher tree" seeds by group members. *Behaviour* **154**, 403–411 (2017).
25. E. T. Frank *et al.*, Wound-dependent leg amputations to combat infections in an ant society. *Curr. Biol.* **34**, 3273–3278.e3 (2024).
26. N. Sato, L. Tan, K. Tate, M. Okada, Rats demonstrate helping behavior toward a soaked conspecific. *Anim. Cogn.* **18**, 1039–1047 (2015).
27. I. B. Bartal *et al.*, Neural correlates of ingroup bias for prosociality in rats. *Elife* **10**, e65582 (2021).
28. I. B. Bartal, J. Decety, P. Mason, Empathy and pro-social behavior in rats. *Science* **334**, 1427–1430 (2011).
29. Z. R. Donaldson, L. J. Young, Oxytocin, vasopressin, and the neurogenetics of sociality. *Science* **322**, 900–904 (2008).
30. M. S. Kurdi, K. A. Theerth, R. S. Deva, Ketamine: Current applications in anesthesia, pain, and critical care. *Anesth. Essays Res.* **8**, 283–290 (2014).
31. V. M. Simón *et al.*, Predicting how equipotent doses of chlorpromazine, haloperidol, sulpiride, raclopride and clozapine reduce locomotor activity in mice. *Eur. Neuropsychopharmacol.* **10**, 159–164 (2000).
32. D. A. Ciraulo, M. Oldham, "Chapter sixteen–Sedative hypnotics" in *The Effects of Drug Abuse on the Human Nervous System*, B. Madras, M. Kuhar, Eds. (Academic Press, Boston, 2014), pp. 499–532.
33. R. Du *et al.*, Empathic contagious pain and consolation in laboratory rodents: Species and sex comparisons. *Neurosci. Bull* **36**, 649–653 (2020).
34. L. Li *et al.*, Dorsal raphe nucleus to anterior cingulate cortex 5-HTergic neural circuit modulates consolation and sociability. *Elife* **10**, e67638 (2021).
35. N. P. Franks, General anaesthesia: From molecular targets to neuronal pathways of sleep and arousal. *Nat. Rev. Neurosci.* **9**, 370–386 (2008).
36. S. Hagihira, Changes in the electroencephalogram during anaesthesia and their physiological basis. *Br. J. Anaesth.* **115**, 27–31 (2015).
37. M. Boly, R. D. Sanders, G. A. Mashour, S. Laureys, Consciousness and responsiveness: Lessons from anaesthesia and the vegetative state. *Curr. Opin. Anaesthesiol.* **26**, 444–449 (2013).
38. Y. E. Wu, W. Hong, Neural basis of prosocial behavior. *Trends Neurosci.* **45**, 749–762 (2022).
39. C. Keysers, E. Knapska, M. A. Moita, V. Gazzola, Emotional contagion and prosocial behavior in rodents. *Trends Cogn. Sci.* **26**, 688–706 (2022).
40. V. Ferretti *et al.*, Oxytocin signaling in the central amygdala modulates emotion discrimination in mice. *Curr. Biol.* **29**, 1938–1953.e6 (2019).
41. D. W. Schulz *et al.*, CP-154,526: A potent and selective nonpeptide antagonist of corticotropin releasing factor receptors. *Proc. Natl. Acad. Sci. U.S.A.* **93**, 10477–10482 (1996).
42. L. W. Hung *et al.*, Gating of social reward by oxytocin in the ventral tegmental area. *Science* **357**, 1406–1411 (2017).
43. B. J. Marlin, R. C. Froemke, Oxytocin modulation of neural circuits for social behavior. *Dev. Neurobiol.* **77**, 169–189 (2017).
44. S. L. Resendez *et al.*, Social stimuli induce activation of oxytocin neurons within the paraventricular nucleus of the hypothalamus to promote social behavior in male mice. *J. Neurosci.* **40**, 2282–2295 (2020).
45. B. L. Roth, DREADDs for neuroscientists. *Neuron* **89**, 683–694 (2016).
46. H. S. Knobloch *et al.*, Evoked axonal oxytocin release in the central amygdala attenuates fear response. *Neuron* **73**, 553–566 (2012).
47. D. Viviani *et al.*, Oxytocin selectively gates fear responses through distinct outputs from the central amygdala. *Science* **333**, 104–107 (2011).
48. Y. J. Li *et al.*, Paraventricular nucleus-central amygdala oxytocinergic projection modulates pain-related anxiety-like behaviors in mice. *CNS Neurosci. Ther.* **29**, 3493–3506 (2023).
49. W. Haubensak *et al.*, Genetic dissection of an amygdala microcircuit that gates conditioned fear. *Nature* **468**, 270–276 (2010).
50. T. Qian *et al.*, A genetically encoded sensor measures temporal oxytocin release from different neuronal compartments. *Nat. Biotechnol.* **41**, 944–957 (2023).
51. P. Tovote, J. P. Fadok, A. Luthi, Neuronal circuits for fear and anxiety. *Nat. Rev. Neurosci.* **16**, 317–331 (2015).
52. A. Lefevre *et al.*, Oxytocinergic feedback circuitries: An anatomical basis for neuromodulation of social behaviors. *Front. Neural Circuits* **15**, 688234 (2021).
53. P. X. Luo *et al.*, Oxytocin receptor behavioral effects and cell types in the bed nucleus of the stria terminalis. *Horm Behav.* **143**, 105203 (2022).
54. M. Janecek, J. Dabrowska, Oxytocin facilitates adaptive fear and attenuates anxiety responses in animal models and human studiespotential interaction with the corticotropin-releasing factor (CRF) system in the bed nucleus of the stria terminalis (BNST). *Cell Tissue Res.* **375**, 143–172 (2019).
55. J. Dabrowska *et al.*, Neuroanatomical evidence for reciprocal regulation of the corticotrophin-releasing factor and oxytocin systems in the hypothalamus and the bed nucleus of the stria terminalis of the rat: Implications for balancing stress and affect. *Psychoneuroendocrinology* **36**, 1312–1326 (2011).
56. A. L. Ejdrup *et al.*, Within-mice comparison of microdialysis and fiber photometry-recorded dopamine biosensor during amphetamine response. *ACS Chem. Neurosci.* **14**, 1622–1630 (2023).
57. P. Cao *et al.*, Rescue-like behavior in a bystander mouse toward anesthetized conspecifics promotes arousal via a tongue-brain connection. *Sci. Adv.* **11**, eadq3874 (2025).
58. F. Sun, Y. E. Wu, W. Hong, A neural basis for prosocial behavior toward unresponsive individuals. *Science* **387**, eadq2679 (2025).
59. W. Sun *et al.*, Reviving-like prosocial behavior in response to unconscious or dead conspecifics in rodents. *Science* **387**, eadq2677 (2025).
60. B. Liu *et al.*, Molecular and neural basis of pleasant touch sensation. *Science* **376**, 483–491 (2022).
61. L. Li *et al.*, Dorsal raphe nucleus to anterior cingulate cortex 5-HTergic neural circuit modulates consolation and sociability. *Elife* **10**, e67638 (2021).
62. S. Fang *et al.*, Sexually dimorphic control of affective state processing and empathic behaviors. *Neuron* **112**, 1498–1517.e8 (2024).
63. H. Ueno *et al.*, Rescue-like behaviour in mice is mediated by their interest in the restraint tool. *Sci. Rep.* **9**, 10648 (2019).
64. S. D. Preston, F. B. M. de Waal, Empathy: Its ultimate and proximate bases. *Behav. Brain Sci.* **25**, 1–20 (2002).
65. N. Padilla-Coreano, K. M. Tye, M. Zelikowsky, Dynamic influences on the neural encoding of social valence. *Nat. Rev. Neurosci.* **23**, 535–550 (2022).
66. K. M. Tye, Neural circuit motifs in valence processing. *Neuron* **100**, 436–452 (2018).
67. P. X. Luo *et al.*, Oxytocin receptor behavioral effects and cell types in the bed nucleus of the stria terminalis. *Horm Behav.* **143**, 105203 (2022).
68. F. Althammer, V. Grinevich, Diversity of oxytocin neurons: Beyond magno- and parvocellular cell types? *J. Neuroendocrinol.* **30**, e12549 (2017).
69. M. Gong *et al.*, Dysfunction of inflammation-resolving pathways is associated with postoperative cognitive decline in elderly mice. *Behav. Brain Res.* **386**, 112538 (2020).
70. Y. Q. Yu, D. M. Barry, Y. Hao, X. T. Liu, Z. F. Chen, Molecular and neural basis of contagious itch behavior in mice. *Science* **355**, 1072–1076 (2017).
71. F. Gao *et al.*, A non-canonical retina-ipRGCs-SCN-PVT visual pathway for mediating contagious itch behavior. *Cell Rep.* **41**, 111444 (2022).
72. J. L. Gomez *et al.*, Chemogenetics revealed: DREADD occupancy and activation via converted clozapine. *Science* **357**, 503 (2017).
73. T. Karigo *et al.*, Distinct hypothalamic control of same- and opposite-sex mounting behaviour in mice. *Nature* **589**, 258–263 (2019).
74. J. J. Walsh *et al.*, 5-HT release in nucleus accumbens rescues social deficits in mouse autism model. *Nature* **560**, 589–594 (2018).
75. Y. Yuan *et al.*, Reward inhibits paraventricular CRH neurons to relieve stress. *Curr. Biol.* **29**, 1243–1251.e4 (2019).
76. F. Ali *et al.*, Ketamine disinhibits dendrites and enhances calcium signals in prefrontal dendritic spines. *Nat. Commun.* **11**, 72 (2020).
77. F.-R. Zhang *et al.*, PhotometryAnalyses. Github. https://github.com/FR-ZH/PhotometryAnalyses. Deposited 2 April 2025.